Comparisons of Temporal and Spatial Trends in the Spatially Complete Global Spectral Surface Albedos Products

Eric G. Moody, Michael D. King, *Senior Member, IEEE*, Steven Platnick, Crystal B. Schaaf, *Member, IEEE*

IEEE Transactions on Geoscience and Remote Sensing

Manuscript submitted October 23, 2005.

E. G. Moody is with L-3 Communications Government Services, Inc., Vienna, VA 22180 USA (e-mail: moody@climate.gsfc.nasa.gov).

M. D. King and S. Platnick are with the Earth-Sun Exploration Division, NASA Goddard Space Flight Center, Greenbelt, MD 20771 USA.

C. B. Schaaf is with Center for Remote Sensing, Department of Geography, Boston University, Boston, MA 02215 USA.

Abstract—Five years of spatially complete snow-free land surface albedo data have been prepared using high quality white-sky and black-sky land surface albedo observations (MOD43B3) from the MODIS instrument aboard NASA's Terra satellite platform. The data were generated using an updated ecosystem-dependant temporal interpolation technique.

In this paper, we describe the refinements in the technique and the creation of a spatially complete snow-free five-year aggregate climatology product. This paper also describes an error analysis of the interpolation technique. The filled albedo products are examined through comparisons of temporal and spatial trends for pixels that have been filled versus pixels that have been retained in the original MOD43B3 values. The variability in the trends showcase how the filling technique maintains the pixel-level spatial, spectral, and temporal integrity of the MOD43B3 data. These comparisons are made for both a single-year of filled data, year 2002, and for the five-year aggregate climatology product.

Index Terms—Ecosystem, modeling, Moderate Resolution Imaging Spectrometer (MODIS), remote sensing, satellite applications, spectral surface albedo, Terra, vegetation phenology.

I. INTRODUCTION

Among inputs into various earth system modeling and remote sensing efforts, spatially complete snow-free land surface albedo data are critical as they describe the radiative properties of the earth's surface. Albedo represents the ratio of reflected to incoming solar radiation at the earth's surface. It has proven to be important for a variety of projects including the remote sensing of cloud properties [13], [15], [16], [20], atmospheric aerosol [6], [11], [14] properties from space, the ground-based analysis of aerosol optical properties from surface-based sun/sky radiometers [3], [5], biophysically-based land surface modeling of the exchange of energy, water, momentum, and carbon for various land use categories [1], [25], and studies of surface energy balance [2], [7], [28]. The modeling community requires values of snow-free surface albedo to initialize their models and therefore needs remotely sensed data that have had all ephemeral and seasonal snow effects removed.

Since February 24, 2000, the Moderate Resolution Imaging Spectroradiometer (MODIS) onboard NASA's Terra [12] spacecraft has been observing diffuse bihemispherical (white-sky) and direct beam directional hemispherical (black-sky) land surface albedo data, known as MOD43B3 [22]. This data product provides global values every 16 days at 1 km spatial resolution for the first seven MODIS bands, 0.47 through 2.1 μm, and for three broadband wavelengths, 0.3-0.7, 0.3-5.0, and 0.7-5.0 μm. The products have been validated [8], [9], [17], [26] and the recent collection 4 reprocessed data are distinguished as "Validated – Stage 1".

As described in Moody et al. [18], roughly 30% of the global land surface on an annual equal-angle basis is obscured due to persistent and transient cloud cover, while another 20% is obscured due to ephemeral and seasonal snow ef-

fects. To provide researchers with a spatially complete global snow-free land surface albedo dataset that they require, an ecosystem-dependant temporal interpolation technique was developed to fill missing or lower quality data and snow covered values from the official MOD43B3 dataset with geophysically realistic values. The technique is based upon the concept that within a limited region, pixels of the same ecosystem classification should exhibit roughly the same phenological, or temporal, behavior [10], [19], [21], [23], [24], [27], [29]. Variations in climate and soil conditions, however, result in pixel-to-pixel differences in the relative magnitudes of the behavioral curves. In order to maintain these spatial pixel-level variations in a temporal sense, missing data are filled in by imposing the shape of the pixel's ecosystem classification phenological curve onto any temporal data that does exist for that pixel. Moody et al. [18] showed that this technique replaces missing data with values that have only 3-8% error.

The purpose of the present paper is to refine and apply the ecosystem-dependent temporal interpolation technique to five years of collection 4 MOD43B3 albedo data, years 2000-2004. This will provide researchers with snow-free spatially complete land surface albedo data matching the five years of to-date MODIS operations and provide the inter-annual variability required for detailed studies. In addition, the technique is applied to a five-year aggregate of MOD43B3 data to provide researchers with a climatology, or average year.

This paper builds upon the error analysis presented in Moody et al. [18] by investigating the spatially compete products through comparing temporal and spatial trends of pixels that have been filled in versus pixels flagged as original MOD43B3 data. The variability in the trends will showcase how the temporal interpolation technique maintains the pixel-level integrity of the albedo product. These comparisons will be made for a single-year of filled data, year 2002, and

for the five-year aggregate climatology product.

II. Spatially Complete Products

The spatially filling algorithm has been refined to better describe high latitude areas impacted by seasonal snow and tropical regions with few observations. An updated MODIS International Geosphere-Biosphere Programme (IGBP) ecosystem classification dataset [4], referred to as product MOD12Q1 (annual Collection 4, year 2001, day 001) is used that, among other improvements, has dramatically improved areas classified as urban ecosystem.

The following subsections will describe the refinement of the fill methodology, as applied to the five-year aggregate climatology, and the inclusion of statistics from the aggregate climatology to assist in processing areas of few observations in the five individual years.

A. Refinements in the Fill Methodology

As described in Moody et al. [18], the MOD43B3 data are projected onto a 1′ equal angle grid and further conditioned to remove pixels of lesser quality and pixels flagged as snow. Statistics are computed from the resulting snow-free and high quality albedo data and are used to generate ecosystem dependent local and regional phenological behavior. The interpolation technique is then applied to each pixel by imposing the shape only, not the magnitude, of the appropriate phenological behavior onto any existing pixel-level data. The pixel's missing temporal data are then filled with the selected local-to-regional phenological behavior that best represents the pixel's temporal information.

While the application of the technique is effective in general, proper description of the full dormant state of high latitude Northern Hemisphere winter pixels remains elusive. In these areas, the dormant state is often obscured due to cloud

cover and snow onset, even for local and regional statistics. To approximate the wintertime cycle, the technique described by Moody et al. [18] computes the snow-free yet fully dormant value as a percentage of the summer extreme for each ecosystem class. The last winter 16-day period is then set to this computed value and the temporal behavior is prescribed.

Unfortunately, snow contaminated albedo values and the least-squares polynomial fit calculation can result in unphysical dormant states. The majority of these anomalies occur in the early through late winter time period. To resolve this issue, the phenological behavior is screened to ensure physical behavior. For each fitted phenological curve, the winter and late spring/early fall mean values are computed from three winter 16-day periods (either periods 65-97 or 289-321) and three late spring/early fall 16-day periods (either periods 129-161 or 225-257). A percentage change is computed and compared to the percentage of the summer extreme value. If the trends are opposite, then the curve is removed from consideration as it is deemed to be decaying in an unphysical manner.

Additional refinements include using the five-year aggregate MOD43B3 data in areas of limited temporal coverage (i.e. high latitude snow-covered areas and tropical regimes). The added temporal coverage of these statistics provides more robust description of the temporal behavior.

B. *Five-Year Aggregate Climatology Product*

The spatially complete five-year (2000-2004) aggregate climatology product is generated by first aggregating the highest quality snow-free MOD43B3 retrievals. For each pixel in each 16-day period, an average is computed for valid data from each of the five years. The resulting snow-free aggregate dataset is comprised of white- and black-sky albedo for 23 16-day periods, from days 001

to 353, for each of the original 10 bands in the MOD43B3 product.

Ecosystem-dependent local and regional statistics of the winter percentage of the summer extreme values for each ecosystem class are computed from the aggregate MOD43B3 data. The refined temporal interpolation technique [Moody et al. [18] and discussed in Section IIA] is then applied to these data to generate the spatially complete five-year aggregate climatology.

C. *Single-Year Product*

The five single-year MOD43B3 data (2000, 2001, ..., 2004) are likewise processed with the refined temporal interpolation technique to provide 5 consecutive years of spatially complete albedo data. In addition to the refinements described above, the five-year aggregate MOD43B3 data have been incorporated into the single-year processing to assist in areas with limited temporal coverage. These areas include high latitude snow impacted regions and tropical persistent cloud regions.

As will be described in Section III (Fig. 1), the five-year aggregate MOD43B3 data have better temporal coverage that results in more robust temporal trends. As such, the aggregate MOD43B3 data can be used in three ways. First, in high latitudes, the percentage of the summer extreme albedo computed from a single year is replaced with the five-year aggregate value. Also in northern high latitudes (>40°), each pixel's data during dormant periods (16-day periods beginning on days 001-129 and 241-353) with missing single-year MOD43B3 statistics are replaced with the associated five-year aggregate MOD43B3 statistics. This allows for a more complete description of the dormant state, while still maintaining the integrity of the single-year data.

Pixels in tropical regions have limited and sometimes no temporal coverage

due to persistent or extended seasonal cloud cover. To enhance the spatial fidelity of pixels with no temporal coverage and to provide more robust temporal trends, the five-year aggregate tropical statistics are substituted for the single-year tropical statistics. Although the unique inter-annual magnitude of each pixel's temporal trend will be maintained, the inter-annual temporal variability may be curtailed in tropical areas that rely upon these statistical instead of pixel-level trends.

Processing of year 2000 data also requires special attention, as data for the first three 16-day periods (001, 017, and 033) are not available as the Terra satellite was not yet operational. As the temporal interpolation technique requires a full year's worth of data to process, the five-year aggregate data and statistics are substituted directly for these three periods.

III. Trend Comparisons of Filled and Original MOD43B3 Pixels

Error analysis of the spatially complete albedo products was performed in Moody et al. [18] by comparing artificially filled values with the values actually retrieved. This paper builds upon this work by comparing temporal and spatial trends of pixels that have been filled in the spatially complete product versus the temporal and spatial trends of pixels flagged as original MOD43B3 data. The variability in the trends will showcase how the temporal interpolation technique maintains the pixel-level integrity of the albedo product. These comparisons will be made for both a single-year of filled data, year 2002, and for the five-year aggregate climatology product. While there will be interannual variations in any of the single-year products, analysis on a single year (2002) will provide an example of trends associated with the other years.

Processing Quality Assurance (QA) of the spatially complete albedo product

records whether a pixel's MOD43B3 data were of high enough quality to be preserved or if they were filled using the temporal interpolation technique. Through this QA, statistics are computed for both pixels flagged as original MOD43B3 data and filled data. Trends are computed from the white-sky albedo data by ecosystem class, latitude belt, and 16-day period, as well as by global and yearly quantities.

A. Spatial and Temporal Variability in Percentage of Pixels Filled

The location and percentage of pixels that are filled varies both temporally and spatially. These variations can be explored through an investigation of the percentage of pixels filled, or the number of pixels filled divided by the total number of pixels. Examining these trends can provide a sense of where on the globe there is better temporal coverage that will thereby provide better phenological information for performing the temporal interpolation to fill missing data. While each band will have it's own unique number and location of pixels filled, the variability between bands is very minor. As such, data from the 0.858 μm band will be used for illustration of these trends.

To provide an overall sense of global yearly temporal coverage, Fig. 1 illustrates the number of 16-day periods that a pixel has maintained its original MOD43B3 data. Fig. 1a shows that the 2002 single-year product has limited temporal coverage in persistently cloudy regions (tropics, Southeast Asia, India) and the seasonally snow-impacted areas (Northern Hemisphere mid to high latitudes) in which the snow-free dormant state is not always observed. Some areas (in grey) have no observations at all for the entire year. Fig. 1b, the five-year aggregate climatology, shows dramatic improvements in the overall temporal coverage compared to the 2002 product. This is especially true in areas with limited or no coverage (cloud and snow-impacted areas). This increase in

or no coverage (cloud and snow-impacted areas). This increase in temporal coverage can lead to improved description of the phenological behavior.

Global trends of where and when pixels are most likely to be filled are illustrated in Figs. 2a and 2b, respectively. Fig. 2a shows yearly statistics computed by 10° latitude belts, and confirms that snow-impacted and seasonally or persistently cloudy areas have the largest number of filled pixels, whereas mid-latitude pixels predominantly retain their original MOD43B3 data. The region with the best MOD43B3 data coverage is the 20°-40°S zone, a belt containing central and southern Australia, southern Africa, and south-central South America. This is because, with the exception of parts of South America and Africa, this region falls predominantly within the arid ecosystems of deserts and shrublands. For the aggregate climatology, this area consists of nearly all MOD43B3 pixels, with only a fraction of a percent to a few percent containing filled pixels.

Unsurprisingly, Fig. 2b, which reveals global statistics computed for each 16-day period, demonstrates that the beginning and end of the year has the highest overall percentage of filled pixels due to the impact of seasonal snow. The middle of the year has the highest percentage of available MOD43B3 pixels with the tropical regions accounting for the majority of the filled pixels. For any 16-day period, the climatology has 10-20% more MOD43B3 pixels than the single-year data. On a yearly global basis, the climatology has 32% of it's pixels filled compared to 47% of the single-year data.

Fig. 3 shows histograms of global yearly percentage of pixels filled by ecosystem class, highlighting which ecoclasses are filled the most often. The variability is primarily due to climatology and the global distribution of classes. It is not surprising to find that arid classes (desert, closed shrubs, permanent snow) require the least amount of filling, whereas classes predominantly in the tropics

(evergreen broadleaf forest, wetlands) require the most filling of pixels. Of the forest classes, the deciduous broadleaf forest has the best coverage, primarily due to the majority of these pixels residing in the 50°-30°N and 10°-30°S latitude belts. The aggregate climatology dramatically improves the coverage of classes within the broader 50°-20°N and 10°-40°S latitude belts (deciduous broadleaf forest, cropland, crop mosaic, urban, savanna, grassland, and closed shrubs).

To provide a more in-depth analysis, statistics from three selected ecosystem classes were explored. Fig. 4 shows the percentage of pixels that were filled in for cropland, grassland, and mixed forest. These ecosystems were selected because they have distinct phenological behavior and a wide range of maximum and minimum albedo values due to growth of the vegetation canopy. Figs. 4a-c show yearly percentages of filled pixels by 10° latitude belts, whereas Figs. 4d-f show percentage of pixels filled for 16-day trends over the latitude belt covering 50°-40°N. These analyses serve to showcase the full variability in spatial and temporal MOD43B3 coverage.

The yearly trends by 10° latitude belts shown in Figs. 4a-c exhibit similar patterns for each of the three ecosystem classes. There are large amounts of filled pixels in the equatorial and high latitude zones, and conversely there are large percentages of original MOD43B3 pixels in the mid-latitudes. All exhibit local maxima in the number of filled pixels in the 30°-20°N latitude belt, primarily due to extended rain periods with persistent and seasonal clouds in India and Southeast Asia. This is especially true for cropland, which is primarily contained in this region of that latitude belt. Again, the aggregate climatology consists of nearly all MOD43B3 pixels in the 20°-40°S latitude belt due to climatology and distribution of ecoclasses.

Examining the temporal trends for the 50°-40°N latitude belt, shown in Figs.

4d-f, reveal that the three ecoclasses exhibit trends with a high percentage of filled pixels at the beginning and end of the year due primarily to seasonal snow. While the 2002 single-year data exhibit interannual variability in seasonal snow effects, the averaging nature of the five-year climatology has dampened interannual variability. For this particular latitude belt, Grassland appears to be the least snow-covered ecosystem during the winter periods. Overall, the aggregate climatology is less impacted by snow during these times of year and once again consists almost entirely of MOD43B3 pixels in the middle of the year. Some 16-day periods have less than one percent of filled pixels during the middle of the year, especially grasslands from periods starting at days 161 to 265.

B. *Spatial and Temporal Variability in White-Sky Albedo*

The radiative properties of a snow-free surface are primarily dependent on the ecosystem classification (ground and vegetation canopy properties) and local climatology. Spatial variability in surface properties arises both from the distribution of ecosystems, as well as the local climatology, and thereby condition of the vegetation. A pixel's radiative properties change temporally based on seasonal climatic and vegetative conditions. Vegetative surfaces exhibit defined phenological growth patterns, however interannual variability in climate can curtail or extend periods of productive vegetation. These factors contribute to the spatial and temporal patterns of the white-sky albedo shown in Fig. 5. It is important to note that the averaging nature of the five-year climatology, Figs. 5a, c, e, and g, does not allow for real interannual variability in land-cover changes. This is especially true for interannual variability in drought and extended growth seasons.

To check that the fill temporal interpolation technique maintains spatial,

spectral, and temporal integrity, trends of average white-sky albedo are examined for the same selection of ecosystem classes (cropland, grassland, and mixed forest) over the 50°-40°N latitude belt. In addition, the statistics are compiled for three bands (0.47 μm, 0.858 μm, and the shortwave broadband 0.3-5.0 μm) to provide trends over a range of albedo values and spectral characteristics. For example, the near-infrared (0.858 μm) band showcases changes in albedo due to vegetation phenological behavior. White-sky albedo was selected as this is the bihemispherical reflectance under conditions of isotropic illumination and thereby excludes any angular solar effects.

Fig. 6 compares the spatial variability in the single-year (2002) and the aggregate climatology albedo data for a single 16-day period (Day 193, July 12-27) as a function of latitude, separated into 10° latitude belts. For this time of year, there are very few filled pixels in the 10°-40°S latitude belt, with less than 10% filled pixels for single-year processing (2002) and less than 1% for the aggregate climatology. The 0°-40°N latitude belts vary from roughly 40-90% filled pixels for that period from the single-year processing (2002) and 20-70% filled pixels from the aggregate climatology. For the selected ecoclasses and spectral bands, the filled pixels and MOD43B3 pixels have trends that appear consistent with one another. In the near-infrared 0.858μm band, the cropland and mixed forest trends exhibit peak growth in the Northern Hemisphere, and are dormant in the Southern Hemisphere. The peak in the grassland occurs in the 20°-10°N latitude belt when the grassland of this region is in full growth as the Intertropical Convergence Zone (ITCZ) brings rain to this region during this time of year.

Some of the trends seen in Fig. 6 in the tropical latitudes are slightly divergent between MOD43B3 and filled pixels. This is mainly due to the limited number of filled pixels in this region, as shown in Fig. 4, and the fact that the pix-

els are dispersed over 3 continents having different climatic conditions. For example, grassland is present on all 3 continents in these latitudes. The filled pixels, however, primarily occur in South America and Northern Australia, whereas the MOD43B3 pixels are primarily from southern Africa. As the ITCZ is in northern Africa, the African grassland is senescent whereas the other continents are not as much in decay, especially the subtropical northern Australian pixels. The resulting anomaly between MOD43B3 and filled pixels across the regions highlights the strength of the fill methodology. The methodology is able to maintain the unique phenological state and thereby the integrity of each local and regional area.

The temporal variability in the single-year (2002) and aggregate climatology albedo data also can be examined by computing mean albedo values within the 50°-40°N latitude belt. Fig. 7 shows the white-sky albedo as a function of 16-day time period for each of the 23 time periods and for each of three ecosystems. A cursory examination of the temporal trends shows that the MOD43B3 and filled pixels exhibit similar annual behavior, with the maximum vegetative growth and dormant states appearing in good agreement (0.858 μm band best shows the vegetative trends) for both the single-year and aggregate climatology data. A closer inspection revels that there are some discrepancies in January and February (e.g., climatology and 2002 grassland, Figs. 7c and d, respectively) as well as in July and August (e.g. Figs 7e and f). As will be explained, these arise from small sample sizes of MOD43B3 and filled pixels, respectively.

To begin to explain these discrepancies, it is important to note that the 50°-40°N latitude belt is distributed across three continents. Due to differences in local climatology and vegetative/ground structure, these regions can have varying albedo magnitudes (dormant and mature) within the same ecosystem class, as

shown in Fig. 5. With a (large or small) sample that is evenly distributed across a latitude belt, these local variances can be dampened and a latitudinal mean trend is observed. However, when one region is disproportionately represented, the average value for the latitude belt is skewed towards that region's value. This is exacerbated when there is a small sample size and one region is wholly overrepresented.

Referencing Fig. 4 , most of the anomalies seen in Fig. 6 occur during periods when either filled (winter 2002) or MOD43B3 (summer aggregate climatology) pixels dominate. This results in a small sample of MOD43B3 or filled pixels, respectively, from which the latitudinal statistics are computed. When examined, these small samples tend to predominantly come from a single, isolated, and specific region. These regions tend to have magnitudes (dormant or mature) that differ substantially from the average across all pixels (MOD43B3 and filled) of the same ecosystem class in the latitude belt. As a result, the latitudinal mean albedo values computed from these small samples differ from the majority trend and thereby create these anomalies. On a positive note, these anomalies provide examples of how the temporal interpolation technique maintains the spatial and temporal integrity of the data. It also demonstrates the spatial and temporal resolution of the MOD43B3 data.

Sample size also impacts the overall smoothness of the trends. For example, the MOD43B3 pixel temporal trends in Fig. 7 are much smoother in the summer than the filled pixel trends. This is due to a large MOD43B3 sample size that is evenly distributed across the latitude belt. Conversely, the filled pixels' trends are more jagged during this period as small statistical sizes allow for specific regions to dominate the trend in one time period and other regions to dominate the trend in subsequent time periods.

A specific example of such an anomaly occurs for the grassland ecoclass, Figs 7c and d. In the aggregate climatology's 0.47 μm data, Fig. 7c, there is a deviation between filled and MOD43B3 trends between days 161 and 289 (peaking at day 257). During this time, as seen in Fig. 4e, the filled pixels represent only a fraction of 1% of the total grassland pixels in this latitude belt. In fact, at the peak deviation, day 257, there are 4,420 filled pixels, or about 0.25% of the total grassland pixels in the latitude belt. Of these 4,420 filled pixels, 4,263 pixels (96.5%) reside in a single, small region located in central Asia. This region, however, has a magnitude (0.106) that differs substantially from the MOD43B3 latitudinal average (0.066). As a result, the filled pixel latitudinal trend deviates from the MOD43B3 latitudinal trend during this time period. This demonstrates that the spatial and temporal uniqueness of this region is maintained in the temporal interpolation technique used to fill the missing data.

Conversely, during the winter, grasslands from the 0.858 μm 2002 single-year processed data, Fig. 7d, primarily consist of filled pixels. Examining Fig. 7d, the MOD43B3 pixels' trend in the beginning of the year is out of phase with the filled pixels' trend, with maximum deviation occurring around period 017. During this period, only 7.086% of the latitude belt's pixels are from original MOD43B3 data. Upon closer inspection, a majority (72.1%) of these MOD43B3 pixels reside in a single region located in eastern Asia. This region is in a dormant state whose magnitude is higher (0.260) than the latitudinal average filled pixel state (0.208). The pixels from this area dominate the statistical computation, resulting in the MOD43B3 trend being out-of-phase with the filled pixel trend. This demonstrates that the original MOD43B3 data also have fine spatial and temporal resolution.

IV. CONCLUSIONS

Snow-free land surface albedo is an important parameter in various Earth system modeling initiatives and remote sensing and radiative transfer projects. Five years of white-sky and black-sky land surface albedo observations from the MODIS instrument aboard NASA's Terra satellite (MOD43B3) have provided researchers with a climatology of the Earth's radiative properties at fine spatial, spectral, and temporal resolutions. Missing data in the five years (2000-2004) of the MOD43B3 product, due to cloud cover and the presence of ephemeral seasonal snow, have been filled using an ecosystem-dependant temporal interpolation technique first reported in Moody et al. [18].

In this paper, we describe refinements in the technique that address areas of limited observation, namely persistently cloudy (tropical) and snow-impacted (high latitude) regions. Also described is the creation of a spatially complete snow-free five-year aggregate climatology product. For this product, five years of high quality MOD43B3 observations are aggregated for each of the yearly 23 16-day time periods. The remaining missing values are filled using the refined temporal interpolation technique.

Error analysis of the interpolation technique was performed in Moody et al. [18]. This paper builds upon this work by comparing temporal and spatial trends of pixels that have been filled in the spatially complete product versus pixels flagged as original MOD43B3 data. The variability in the trends showcase how the filling technique maintains the pixel-level spatial, spectral, and temporal integrity of the MOD43B3 data. These comparisons are made for a single-year of filled data, year 2002, and for the five-year aggregate climatology product.

ACKNOWLEDGMENTS

The research reported in this article was supported by the MODIS Science Team under NASA contract 621-30-H4 to Goddard Space Flight Center (EGM, MDK, SP) and NASA contract NAS5-31369 to Boston University (CBS). The authors would like to express their appreciation to Dr. Lahouari Bounoua, NASA Goddard Space Flight Center, for providing valuable insight into modeling community requirements and reviewing the methodologies used in this work.

REFERENCES

[1] L. Bounoua, R. DeFries, G. J. Collatz, P. Sellers, and H. Khan, "Effects of land cover conversion on surface climate," *Climatic Change*, vol. 52, pp. 29-64, 2002.

[2] P. A. Dirmeyer and J. Shukla, "Albedo as a modulator of climate response to tropical deforestation," *J. Geophys. Res.*, vol. 99, pp. 20863-20878, 1994.

[3] O. Dubovik, A. Smirnov, B. N. Holben, M. D. King, Y. J. Kaufman, T. F. Eck, and I. Slutsker "Accuracy assessments of aerosol optical properties retrieved from AERONET sun and sky-radiance measurements," *J. Geophys. Res.*, vol. 105, pp. 9791-9806, 2000.

[4] M. A. Friedl, D. K. McIver, J. C. F. Hodges, X. Y. Zhang, D. Muchoney, A. H. Strahler, C. E. Woodcock, S. Gopal, A. Schneider, A. Cooper, A. Baccini, F. Gao, and C. Schaaf, "Global land cover mapping from MODIS: Algorithms and early results," *Remote Sens. Environ.*, vol. 83, pp. 287-302, 2002.

[5] B. N. Holben, T. F. Eck, I. Slutsker, D. Tanré, J. P. Buis, A. Setzer, E. Vermote, J. A. Reagan, Y. J. Kaufman, T. Nakajima, F. Lavenu, I. Jankowiak, and A. Smirnov, "AERONET—A federated instrument network and data archive for aerosol characterization," *Remote Sens. Environ.*, vol. 66, pp. 1-16, 1998.

[6] N. C. Hsu, S. C. Tsay, M. D. King, and J. R. Herman, "Aerosol retrievals over bright-reflecting source regions," *IEEE Trans. Geosci. Remote Sens.*, vol. 42, pp. 557-569, 2004.

[7] W. J. Ingram, C. A. Wilson, and J. F. B. Mitchell, "Modeling climate change: An assessment of sea ice and surface albedo feedbacks," *J. Geophys. Res.*, vol. 94, pp. 8609-8622, 1989.

[8] Y. Jin, C. B. Schaaf, F. Gao, X. Li, A. H. Strahler, W. Lucht, and S. Liang,

"Consistency of MODIS surface bidirectional reflectance distribution function and albedo retrievals: 1. Algorithm performance", *J. Geophys. Res.*, vol. 108 (D5), doi:10.1029/2002JD002803, 2003a.

[9] Y. Jin, C. B. Schaaf, C. E. Woodcock, F. Gao, X. Li, A. H. Strahler, W. Lucht, and S. Liang, "Consistency of MODIS surface bidirectional reflectance distribution function and albedo retrievals: 2. Validation", *J. Geophys. Res.*, vol. 108 (D5), doi:10.1029/2002JD002804, 2003b.

[10] J. Kaduk and M. Heimann, "A prognostic phenology scheme for global terrestrial carbon cycle models," *Climate Research*, vol. 6, pp. 1-19, 1996.

[11] Y. J. Kaufman, D. Tanré, L. A. Remer, E. F. Vermote, A. Chu, and B. N. Holben, "Operational remote sensing of tropospheric aerosol over land from EOS moderate resolution imaging spectroradiometer," *J. Geophys. Res.*, vol. 102, pp. 17051-17067, 1997.

[12] M. D. King, and D. D. Herring, "Monitoring Earth's vital signs," *Sci. Amer.*, vol. 282, pp. 72-77, 2000.

[13] M. D. King, Y. J. Kaufman, W. P. Menzel, and D. Tanré, "Remote sensing of cloud, aerosol, and water vapor properties from the Moderate Resolution Imaging Spectrometer (MODIS)," *IEEE Trans. Geosci. Remote Sens.*, vol. 30, pp. 2-27, 1992.

[14] M. D. King, Y. J. Kaufman, D. Tanré, and T. Nakajima, "Remote sensing of tropospheric aerosols from space: Past, present, and future," *Bull. Amer. Meteor. Soc.*, vol. 80, pp. 2229-2259, 1999.

[15] M. D. King, W. P. Menzel, Y. J. Kaufman, D. Tanré, B. C. Gao, S. Platnick, S. A. Ackerman, L. A. Remer, R. Pincus, and P. A. Hubanks, "Cloud and aerosol properties, precipitable water, and profiles of temperature and humidity from MODIS," *IEEE Trans. Geosci. Remote Sens.*, vol. 41, pp. 442-458, 2003.

[16] M. D. King, S. Platnick, P. Yang, G. T. Arnold, M. A. Gray, J. C. Riédi, S. A. Ackerman, and K. N. Liou, "Remote sensing of liquid water and ice cloud optical thickness and effective radius in the arctic: Application of airborne multispectral MAS data," *J. Atmos. Oceanic Technol.*, vol. 21, pp. 857-875, 2004.

[17] S. L. Liang, H. L. Fang, M. Z. Chen, C. J. Shuey, C. Walthall, C. Daughtry, J. Morisette, C. Schaaf, and A. Strahler, "Validating MODIS land surface reflectance and albedo products: Methods and preliminary results," *Remote Sens. Environ.*, vol. 83, pp. 149-162, 2002.

[18] E. G Moody, M. D. King, S., Platnick, C. B. Schaaf, and F. Gao, "Spatially complete global spectral surface albedos: Value-added datasets derived from Terra MODIS land products," *IEEE Trans. Geosci. Remote Sens.*, vol. 43, pp. 144–158, 2005.

[19] J. Penuelas, I. Filella, X. Zhang, L. Llorens, R. Ogaya, F. Lloret, P. Comas, M. Estiarte, and J. Terradas, "Complex spatiotemporal phenological shifts as a response to rainfall changes," *New Phytologist*, vol. 161, pp. 837-846, 2004.

[20] S. Platnick, M. D. King, S. A. Ackerman, W. P. Menzel, B. A. Baum, J. C. Riédi, and R. A. Frey, "The MODIS cloud products: Algorithms and examples from Terra," *IEEE Trans. Geosci. Remote Sens.*, vol. 41, pp. 459-473, 2003.

[21] B. C. Reed, J. F. Brown, D. VanderZee, T. R. Loveland, J. W. Merchant, and D. O. Ohlen, "Measuring phenological variability from satellite imagery," *J. Veg. Sci.*, vol. 5, pp. 703-714, 1994.

[22] C. B. Schaaf, F. Gao, A. H. Strahler, W. Lucht, X. W. Li , T. Tsang, N. C. Strugnell, X. Y. Zhang, Y. F. Jin, J. P. Muller, P. Lewis, M. Barnsley, P. Hobson, M. Disney, G. Roberts, M. Dunderdale, C. Doll, R. P. d'Entremont, B. X. Hu, S. L. Liang, J. L. Privette, and D. Roy, "First operational BRDF, albedo

nadir reflectance products from MODIS," *Remote Sens. Environ.*, vol. 83, pp. 135-148, 2002.

[23] M. D. Schwartz, "Green-wave phenology," *Nature*, vol. 394, pp. 839-840, 1998.

[24] M. D. Schwartz and B. C. Reed, "Surface phenology and satellite sensor-derived onset of greenness: An initial comparison," *Int. J. Remote Sens.*, vol. 20, pp 3451-3457, 1999.

[25] P. J. Sellers, D. A. Randall, G. J. Collatz, J. A. Berry, C. B. Field, D. A. Dazlich, C. Zhang, and L. Bounoua, "A revised land surface parameterization (SiB2) for atmospheric GCMs. Part 1: Model formulation," *J. Climate*, vol. 9, pp. 676-705, 1996.

[26] K. Wang, J. Liu, X. Zhou, M. Sparrow, M. Ma, Z. Sun, and W. Jiang, "Validation of the MODIS global albedo surface albedo product using ground measurements in a semidesert region on the Tibetan Plateau", *J. Geophys. Res.*, vol. 109 (D5), doi:10.1029/2003JD004229, 2004.

[27] M. A. White, P. E. Thornton, and S. W. Running. "A continental phenology model for monitoring vegetation responses to interannual climatic variability," *Global Biogeochem. Cycles*, vol. 11, pp. 217-234, 1997.

[28] C. H. Whitlock, T. P. Charlock, W. F. Staylor, R. T. Pinker, I. Laszlo, A. Ohmura, H. Gilgen, T. Konzelman, R. C. DiPasquale, C. D. Moats, S. R. LeCroy, and N. A. Ritchey, "First global WCRP shortwave surface radiation budget data set," *Bull. Amer. Meteor. Soc.*, vol. 76, pp. 905-922, 1995.

[29] X. Zhang, M. A. Friedl, C. B. Schaaf, A. H. Strahler, J. C. F. Hodges, F. Gao, and B. C. Reed, "Monitoring vegetation phenology using MODIS," *Remote Sens. Environ.*, vol. 84, pp. 471-475, 2003.

Eric G. Moody received the B.S. and M.S. degrees in chemical engineering from the Pennsylvania State University in 1996 and 1998, and joined Goddard Space Flight Center through contract with SM&A Corporation (now L-3 Communications Government Services, Inc.).

He has more than 6 years' experience in satellite and aircraft data analysis and evaluation through work with the MODIS Science Team on the development of the cloud optical and microphysical property and Level-3 algorithms, user community software tools, visualization algorithms, and the implementation of ancillary datasets. He also has more then four years experience researching and modeling turbulent fluid dynamics, reaction chemistry, reactor design, and the evolution of particle size distributions through aerosol nucleation and coagulation.

Michael D. King (M'01–SM'03) received the B.A. degree in physics from Colorado College in 1971, and the M.S. and Ph.D. degrees in atmospheric sciences from the University of Arizona in 1973 and 1977, respectively.

He joined NASA Goddard Space Flight Center in January 1978 and is currently Senior Project Scientist of NASA's Earth Observing System (EOS), a position he has held since 1992. He is a member of the MODIS Science Team where he has primary responsibility for developing the cloud optical and microphysical property and Level-3 algorithms. His research experience includes conceiving, developing, and operating multispectral scanning radiometers from a number of aircraft platforms in field experiments ranging from arctic stratus clouds to smoke from the Kuwait oil fires in the Persian Gulf and biomass burning in Brazil and southern Africa.

Dr. King is a Fellow of the American Meteorological Society (AMS), recipient

of the AMS Verner E. Suomi Award for significant and fundamental contributions to remote sensing and radiative transfer, and recipient of the 1992 Transactions Prize Paper Award by the IEEE Geoscience and Remote Sensing Society. He is a member of the US National Academy of Engineering.

Steven Platnick received the B.S. degree in electrical engineering from Duke University in 1979, the M.S. degree in electrical engineering from the University of California Berkeley in 1980, and the Ph.D. degree in atmospheric sciences from the University of Arizona in 1991.

He joined NASA Goddard Space Flight Center in January 2003 and is currently Deputy Project Scientist of NASA's Aqua satellite. Prior to this appointment, he was a Research Associate Professor in the Joint Center for Earth Systems Technology, University of Maryland Baltimore County, a position he held from 1996-2002. He has worked in collaboration with NASA Goddard Space Flight Center since 1993, and prior to that held engineering positions at Hewlett-Packard Co. for 6 years as well as a National Research Council Resident Research Associate position at NASA Ames Research Center. His research experience includes theoretical and experimental studies of satellite, aircraft, and ground-based cloud remote sensing, including applications to MODIS. He is a member of the MODIS Science Team.

Crystal B. Schaaf (M'92) received the S.B. and S.M. degrees in meteorology from the Massachusetts Institute of Technology, Cambridge, in 1982, the M.L.A. degree in archaeology from Harvard University, Cambridge, MA, in 1988, and the Ph.D. degree in geography from Boston University, Boston, MA, in 1994.

She is a Research Associate Professor of Geography and Researcher in the Center for Remote Sensing, Boston University, and is a member of the MODIS

and NPP Science Teams. Her research interests cover remote sensing of land surfaces and clouds, with particular emphasis on surface anisotropy and albedo.

FIGURE LEGENDS

Fig. 1. Number of high quality MOD43B3 retrievals preserved for each pixel in the spatially complete (a) single-year 2002 and (b) five-year (2000-2004) aggregate climatology albedo data. As each year of data is comprised of 23 16-day periods, the maximum is 23. Mid-latitude regions typically have more observations than areas of persistent clouds (tropics) or seasonal snow and low illumination angles (high latitudes). The aggregate product generally provides more complete temporal information than any single year of data.

Fig. 2. Percentage of pixels filled in, given as trends of (a) yearly percentage by 10° latitude belts, and (b) global percentage by day of year. The trends are calculated from the 0.858 μm band for the five-year aggregate climatology and 2002 single-year albedo data.

Fig. 3. Histogram of global yearly percentage of pixels filled in, given by ecosystem class. The statistics are computed from the 0.858 μm band for the five-year aggregate climatology and 2002 single-year albedo data.

Fig. 4. Percentage of pixels filled in, given as trends of (a)-(c) yearly percentage by 10° latitude belts, and (d)-(f) percentage by day of year over the 50°-40°N latitude belt. The trends are computed for three ecosystem classes, cropland (a and d), grassland (b and e), and mixed forest (c and f). The statistics are calculated from the 0.858 μm band for the five-year aggregate climatology and 2002 single-year albedo data.

Fig. 5. Spatially complete white-sky albedo at 0.86 μm for the 16-day periods of (a, b) January 1-16, (c, d) April 3-18, (e, f) July 12-27, and (g, h) September 30-October 14. Data from the five-year (2000-2004) climatology is presented in the left column (a, c, e, g), while the single-year 2002 albedo

data is presented in the right column (b, d, f, h).

Fig. 6. Mean white-sky albedo values computed by 10° latitude belts for three bands (0.47 and 0.858 μm narrowband, and the 0.3-5.0 μm shortwave broadband) during the 16-day period of July 12-27 (data day 193). Trends are computed for three ecosystem classes, cropland (a and b), grassland (c and d), and mixed forest (e and f) from the five-year aggregate climatology (a, c, and e) and the 2002 single-year albedo data (b, d, and f).

Fig. 7. Mean white-sky albedo values computed for each 16-day period for three bands (0.47 and 0.858 μm narrowband, and the 0.3-5.0 μm shortwave broadband) over the 50°-40°N latitude belt. Trends are computed for three ecosystem classes, cropland (a and b), grassland (c and d), and mixed forest (e and f) from the five-year aggregate climatology (a, c, and e) and the 2002 single-year albedo data (b, d, and f).

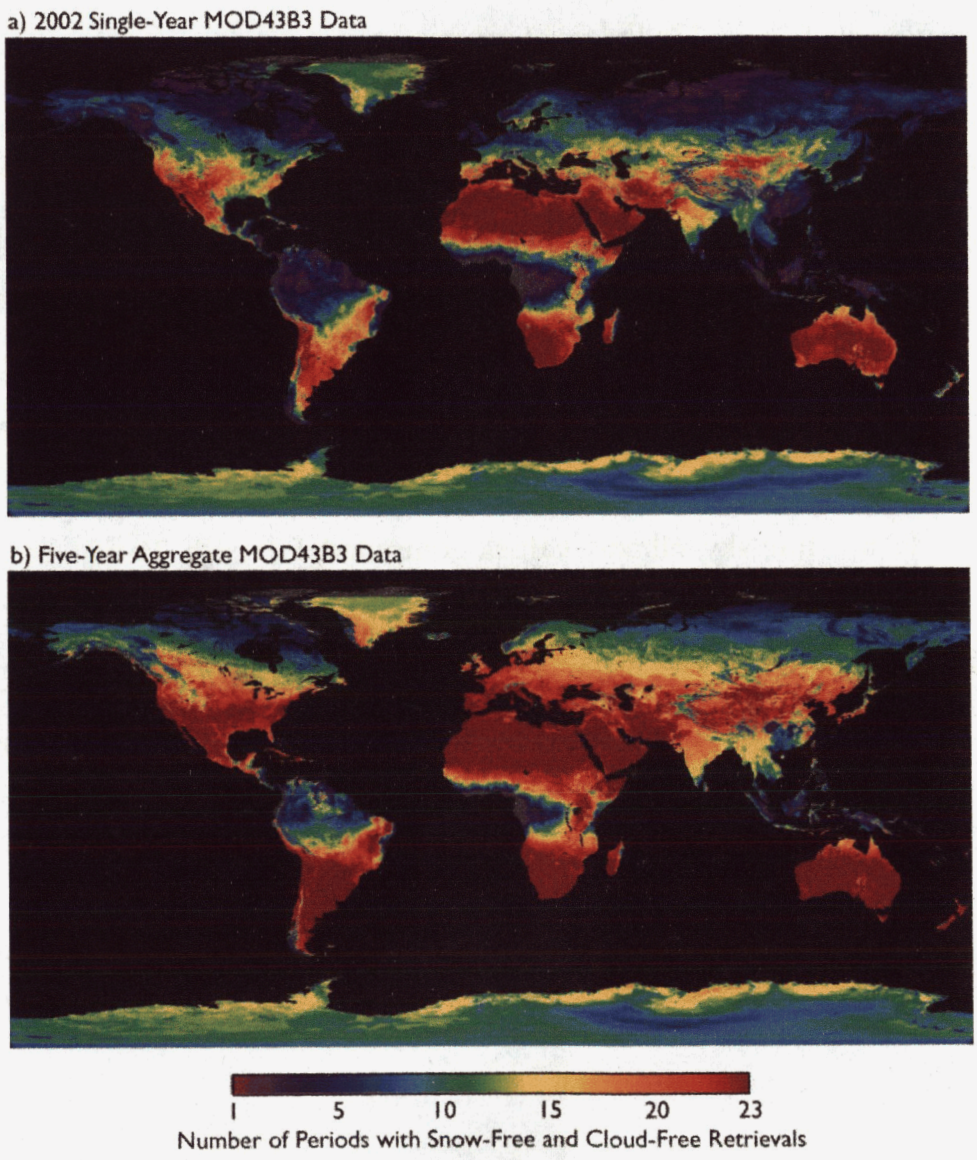

Fig. 1. Number of high quality MOD43B3 retrievals preserved for each pixel in the spatially complete (a) single-year 2002 and (b) five-year (2000-2004) aggregate climatology albedo data. As each year of data is comprised of 23 16-day periods, the maximum is 23. Mid-latitude regions typically have more observations than areas of persistent clouds (tropics) or seasonal snow and low illumination angles (high latitudes). The aggregate product generally provides more complete temporal information than any single year of data.

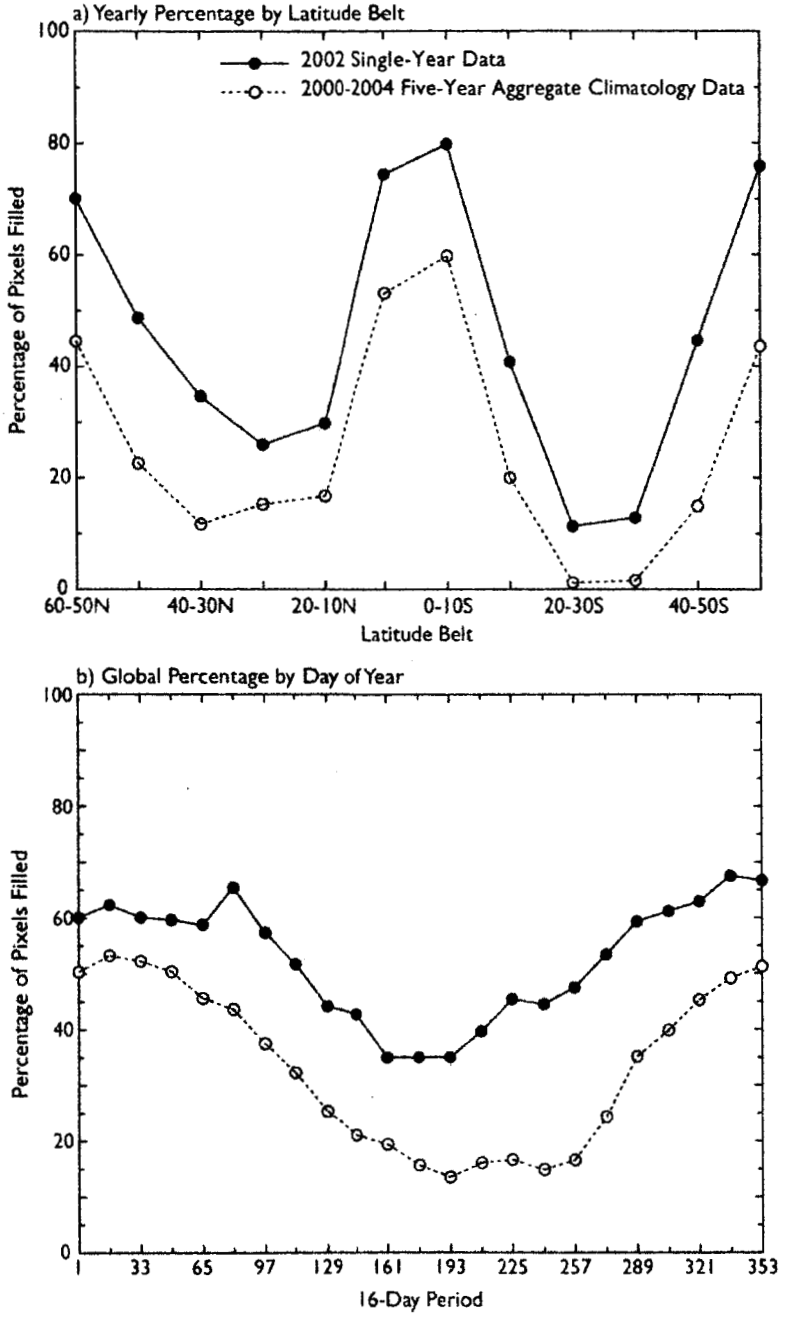

Fig. 2. Percentage of pixels filled in, given as trends of (a) yearly percentage by 10° latitude belts, and (b) global percentage by day of year. The trends are calculated from the 0.858 μm band for the five-year aggregate climatology and 2002 single-year albedo data.

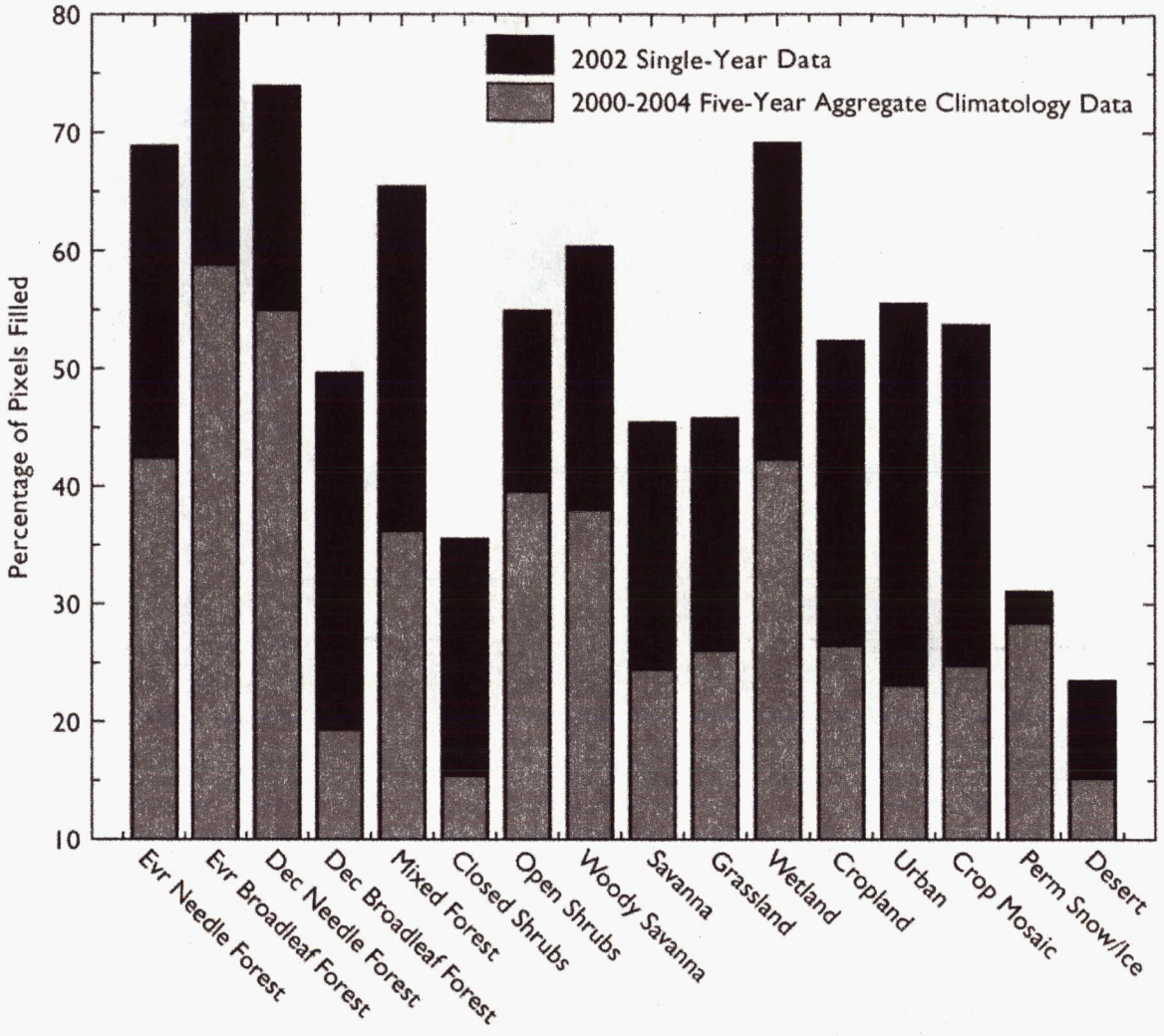

Fig. 3. Histogram of global yearly percentage of pixels filled in, given by ecosystem class. The statistics are computed from the 0.858 μm band for the five-year aggregate climatology and 2002 single-year albedo data.

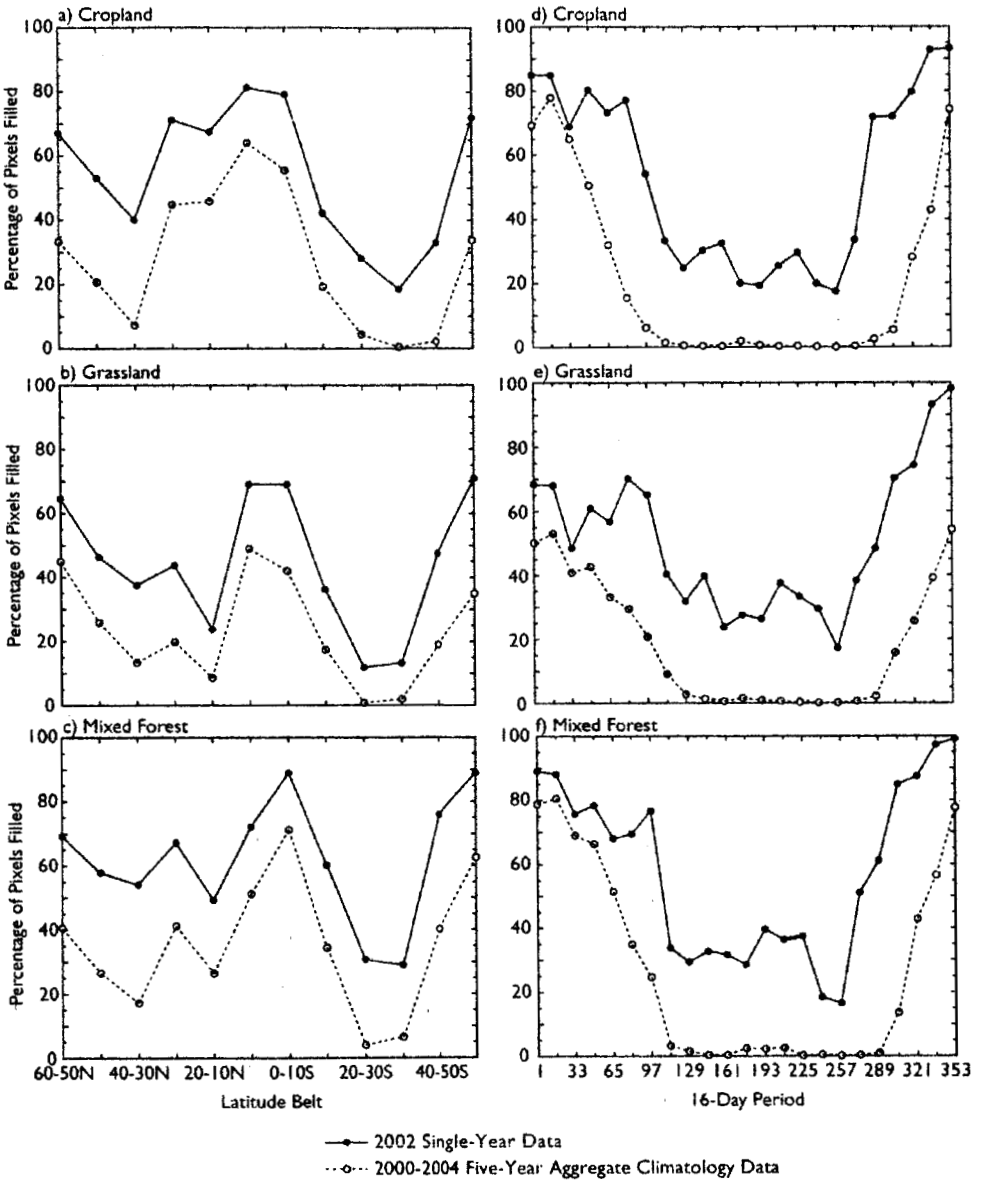

Fig. 4. Percentage of pixels filled in, given as trends of (a)-(c) yearly percentage by 10° latitude belts, and (d)-(f) percentage by day of year over the 50°-40°N latitude belt. The trends are computed for three ecosystem classes, cropland (a and d), grassland (b and e), and mixed forest (c and f). The statistics are calculated from the 0.858 μm band for the five-year aggregate climatology and 2002 single-year albedo data.

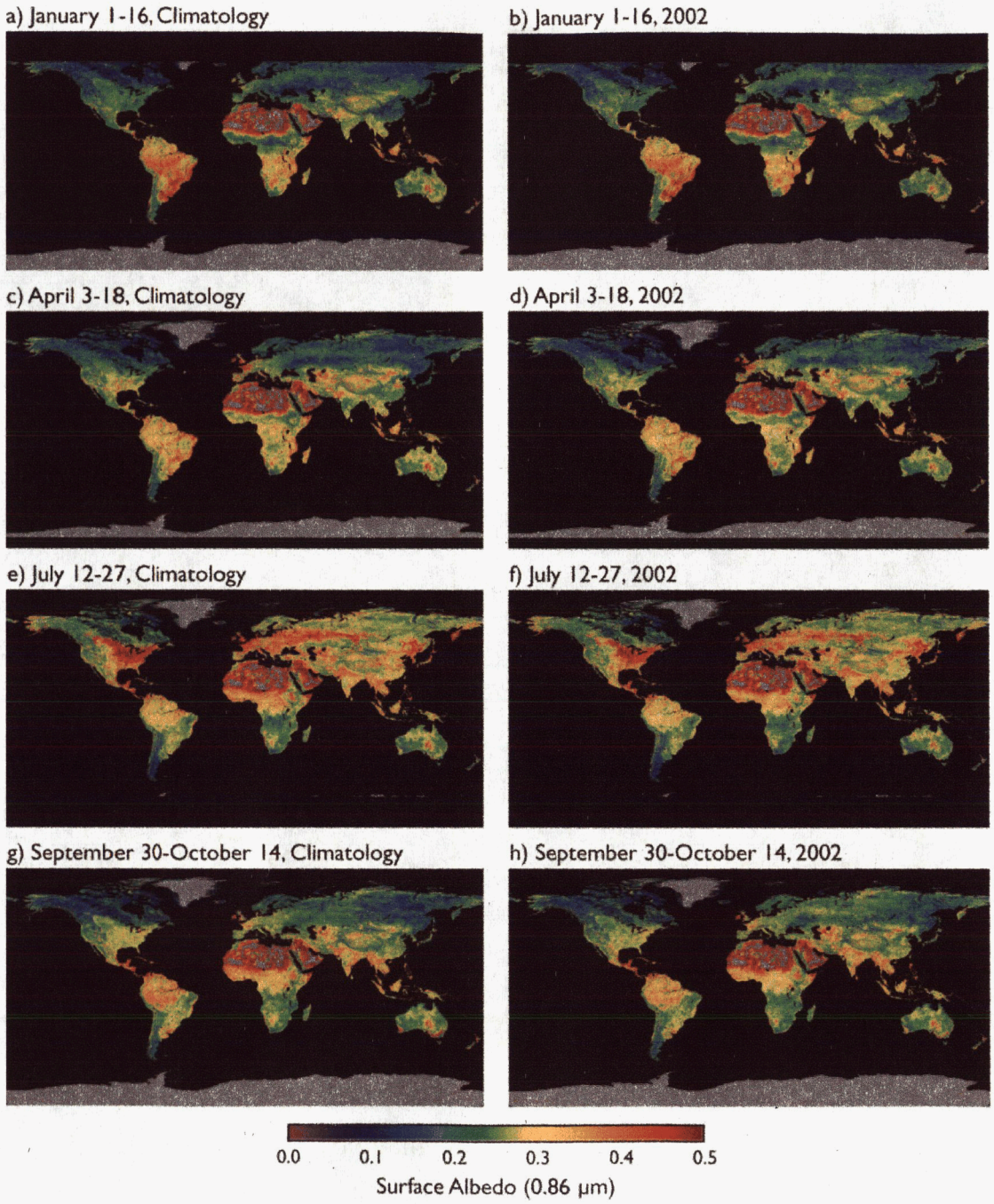

Fig. 5. Spatially complete white-sky albedo at 0.86 μm for the 16-day periods of (a, b) January 1-16, (c, d) April 3-18, (e, f) July 12-27, and (g, h) September 30-October 14. Data from the five-year (2000-2004) climatology is presented in the left column (a, c, e, g), while the single-year 2002 albedo data is presented in the right column (b, d, f, h).

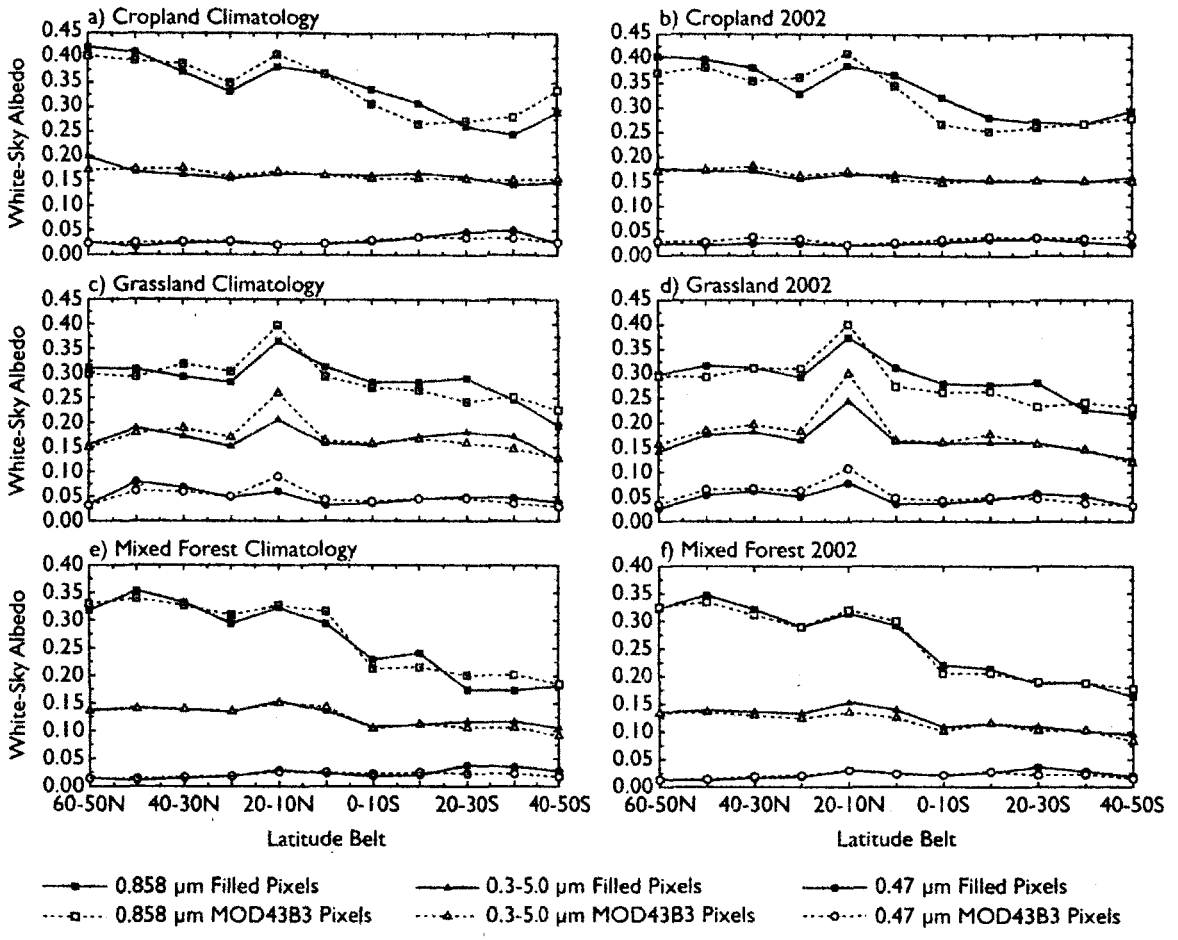

Fig. 6. Mean white-sky albedo values computed by 10° latitude belts for three bands (0.47 and 0.858 μm narrowband, and the 0.3-5.0 μm shortwave broadband) during the 16-day period of July 12-27 (data day 193). Trends are computed for three ecosystem classes, cropland (a and b), grassland (c and d), and mixed forest (e and f) from the five-year aggregate climatology (a, c, and e) and the 2002 single-year albedo data (b, d, and f).

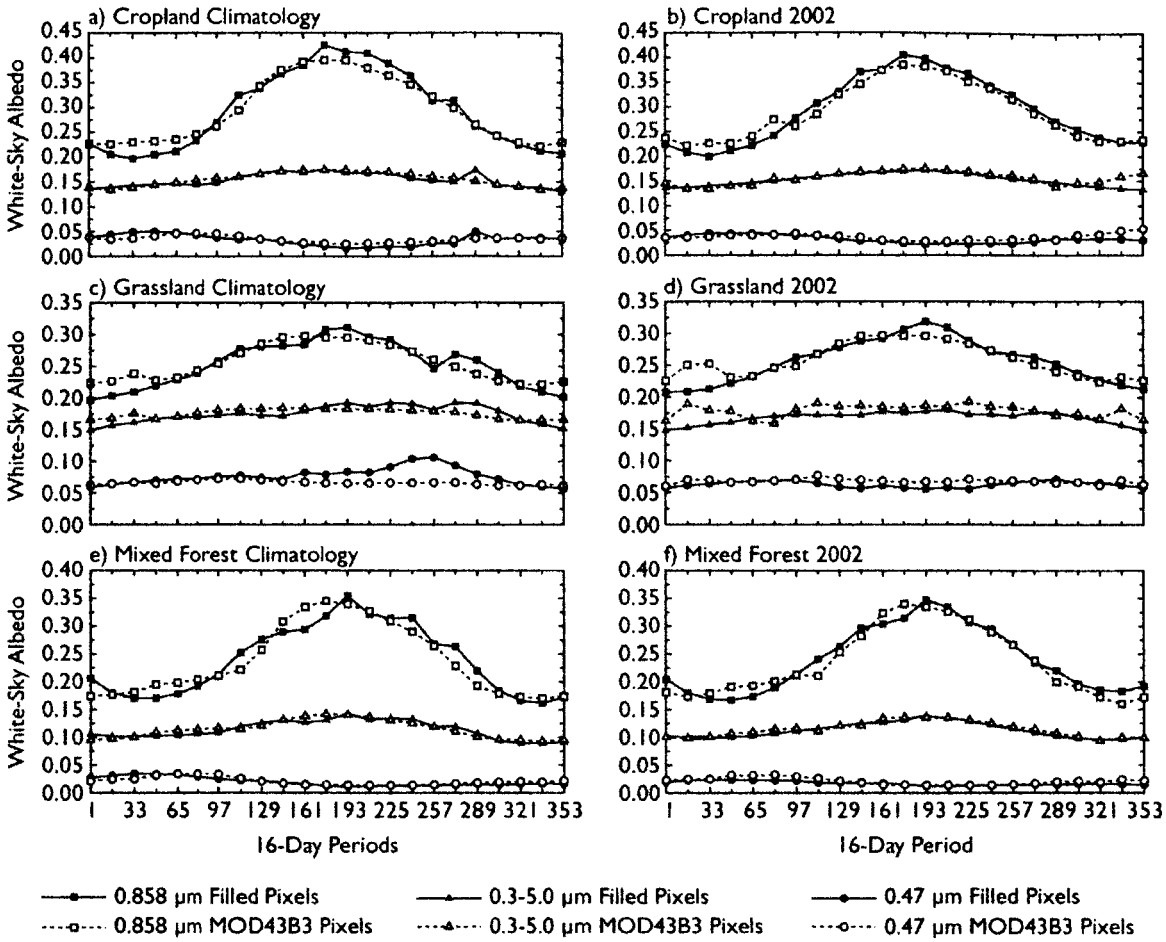

Fig. 7. Mean white-sky albedo values computed for each 16-day period for three bands (0.47 and 0.858 μm narrowband, and the 0.3-5.0 μm shortwave broadband) over the 50°-40°N latitude belt. Trends are computed for three ecosystem classes, cropland (a and b), grassland (c and d), and mixed forest (e and f) from the five-year aggregate climatology (a, c, and e) and the 2002 single-year albedo data (b, d, and f).

Popular Summary of the paper:

Comparisons of Temporal and Spatial Trends in the Spatially Complete Global Spectral Surface Albedos Products

By Eric G. Moody[1], Michael D. King[2], Steven Platnick[2], Crystal B. Schaaf[3]

[1] L-3 Communications Government Services, Inc., Vienna, VA 22180 USA
[2] Earth-Sun Exploration Division, NASA Goddard Space Flight Center, Greenbelt, MD
[3] Center for Remote Sensing, Department of Geography, Boston University, Boston, MA

Among inputs into various Earth system modeling and remote sensing efforts, spatially complete snow-free land surface albedo data are critical as they describe the radiative properties of the Earth's surface. Albedo represents the ratio of reflected to incoming solar radiation at the Earth's surface. It has proven to be important for a variety of projects including the remote sensing of cloud and atmospheric aerosol properties from space, the ground-based analysis of aerosol optical properties from surface-based sun/sky radiometers, biophysically-based land surface modeling of the exchange of energy, water, momentum, and carbon for various land use categories, and studies of surface energy balance. The modeling community requires values of snow-free surface albedo to initialize their models and therefore needs remotely sensed data that have had all ephemeral and seasonal snow effects removed.

The Moderate Resolution Imaging Spectroradiometer (MODIS) onboard the Terra satellite has provided researchers with over five years of validated diffuse bihemispherical (white-sky) and direct beam directional hemispherical (black-sky) land surface albedo observations, known as the MOD43B3 product. This data product provides global values every 16 days at 1 km spatial resolution for the first seven MODIS bands, 0.47 through 2.1 μm, and for three broadband wavelengths, 0.3-0.7, 0.3-5.0, and 0.7-5.0 μm. However, roughly 30% of the global land surface on an annual equal-angle basis is obscured due to persistent and transient cloud cover, while another 20% is obscured due to ephemeral and seasonal snow effects.

To provide researchers with a spatially complete global snow-free land surface albedo dataset that they require, an ecosystem-dependant temporal interpolation technique was previously developed to fill missing or lower quality data and snow covered values from the official MOD43B3 dataset with geophysically realistic values. The purpose of this present paper is to refine and apply the ecosystem-dependent temporal interpolation technique to five years of collection 4 MOD43B3 albedo data, years 2000-2004. This will provide researchers with snow-free spatially complete land surface al-

bedo data matching the five years of to-date MODIS operations and provide the inter-annual variability required for detailed studies. In addition, the technique is applied to a five-year aggregate of MOD43B3 data to provide researchers with a climatology, or average year.

This paper builds upon previously presented error analysis through comparing temporal and spatial trends of pixels that have been filled in versus pixels flagged as original MOD43B3 data. The variability in the trends showcases how the temporal interpolation technique maintains the pixel-level integrity of the MOD43B3 albedo product. These comparisons are made for a single-year of filled data, year 2002, and for the five-year aggregate climatology product.